AGU PUBLICATIONS

Geophysical Research Letters

RESEARCH LETTER
10.1002/2016GL068614

Key Points:
- We apply recently developed models for monitoring of live and dead fuel moisture contents
- We show that the relationship between fuel moisture and wildfire exhibits threshold behavior
- Changes in fuel moisture sufficient to cross critical thresholds can occur over weeks to months

Supporting Information:
- Supporting Information S1
- Figure S1
- Figure S2
- Figure S3
- Table S1

Correspondence to:
R. H. Nolan,
rachael.nolan@uts.edu.au

Citation:
Nolan, R. H., M. M. Boer, V. Resco de Dios, G. Caccamo, and R. A. Bradstock (2016), Large-scale, dynamic transformations in fuel moisture drive wildfire activity across southeastern Australia, *Geophys. Res. Lett.*, *43*, 4229-4238, doi:10.1002/2016GL068614.

Received 8 MAR 2016
Accepted 10 APR 2016
Accepted article online 13 APR 2016
Published online 6 MAY 2016

Large-scale, dynamic transformations in fuel moisture drive wildfire activity across southeastern Australia

R. H. Nolan[1,2,3], M. M. Boer[1], V. Resco de Dios[1,4], G. Caccamo[2,5], and R. A. Bradstock[2]

[1]Hawkesbury Institute for the Environment, Western Sydney University, Richmond, New South Wales, Australia, [2]Centre for Environmental Risk Management of Bushfires, Centre for Sustainable Ecosystem Solutions, University of Wollongong, Wollongong, New South Wales, Australia, [3]Now at Terrestrial Ecohydrology Research Group, School of Life Sciences, University of Technology Sydney, Broadway, New South Wales, Australia, [4]Now at Department of Crop and Forest Sciences-AGROTECNIO Center, Universitat de Lleida, Lleida, Spain, [5]Now at NSW Department of Primary Industries, Parramatta, New South Wales, Australia

Abstract The occurrence of large, high-intensity wildfires requires plant biomass, or fuel, that is sufficiently dry to burn. This poses the question, what is "sufficiently dry"? Until recently, the ability to address this question has been constrained by the spatiotemporal scale of available methods to monitor the moisture contents of both dead and live fuels. Here we take advantage of recent developments in macroscale monitoring of fuel moisture through a combination of remote sensing and climatic modeling. We show there are clear thresholds of fuel moisture content associated with the occurrence of wildfires in forests and woodlands. Furthermore, we show that transformations in fuel moisture conditions across these thresholds can occur rapidly, within a month. Both the approach presented here, and our findings, can be immediately applied and may greatly improve fire risk assessments in forests and woodlands globally.

1. Introduction

Large, high-intensity wildfires pose major threats to people, property, and infrastructure and play a major role in shaping many ecosystems worldwide [*Moritz et al.*, 2014]. The incidence of large wildfires is contingent upon the presence of spatially continuous arrays of plant biomass sufficiently dry to burn, weather conditions conducive to the rapid spread of fire, and the occurrence of ignitions [*Bradstock*, 2010; *Meyn et al.*, 2007]. *Bradstock* [2010] hypothesized that these processes could be characterized as "switches" that have to be synchronously activated for fires to occur. The switch concept implies that there can be transformations in the states of these processes so that rapid shifts between nonflammable and flammable states can occur across large spatial scales.

Evidence for such rapid transformations in biomass (fuel), fuel dryness, and ambient fire weather (high temperatures, strong winds, and low humidity) exist in a variety of ecosystems. Major rainfall events can transform nonflammable deserts by stimulating widespread growth of herbaceous plants, increasing fuel connectivity [*O'Donnell et al.*, 2011; *Turner et al.*, 2008]. Forests are transformed into highly flammable states by the occurrence of major droughts [*Aragao et al.*, 2007; *Bradstock et al.*, 2014], while particular weather systems such as cold fronts, mountain winds, and upper atmospheric instability can cause the rapid onset of severe fire weather [*Hasson et al.*, 2009; *Sharples*, 2009].

In high-biomass ecosystems, such as temperate forests and shrublands, spatially continuous arrays of surface litter and dead and live aerial foliage are ever present, except in the immediate aftermath of fires. The principal preconditions for major wildfires in such ecosystems are therefore the availability of fuel to burn (i.e., its dryness), severe ambient fire weather, and ignitions. Fire danger indices condense information about fire weather and fuel dryness, via drought indices that are assumed to characterize the moisture content of live and dead fuels via a simple index of climatic moisture availability [*Bradshaw et al.*, 1983; *McArthur*, 1967; *Van Wagner*, 1987; *Yebra et al.*, 2013].

Correlations exist between major wildfires and fire danger indices in temperate shrublands [*Verdon et al.*, 2004], but fire danger indices may lack the accuracy and precision for forecasting the timing and locations of highest potential for wildfires. For example, drought indices may not accurately reflect actual moisture values of key fuel elements in these ecosystems because (i) the fuel moisture (FM) of live foliage is dependent upon species-specific attributes, such as rooting depth and drought adaptation strategies, and (ii) the FM of

fine, dead fuels responds to atmospheric conditions [*Caccamo et al*., 2012b; *Resco de Dios et al*., 2015; *Yebra et al*., 2013]. By contrast studies involving direct estimation of either live [*Agee et al*., 2002; *Dennison et al*., 2008] or dead [*Dowdy and Mills*, 2012; *Nash and Johnson*, 1996] FM have indicated the potential for nonlinear relationships between FM and wildfire activity at local to landscape scales [*Jurdao et al*., 2012; *Schoenberg et al*., 2003; *Viegas et al*., 1992]. Thus, thresholds in FM may need to be crossed to provide the potential for the spread of major wildfires, possibly reflecting critical levels of connectivity of dry patches across landscapes [*Caccamo et al*., 2012b].

The ability to forecast wildfire risk at large scales, across varying terrain and vegetation communities, will therefore depend on the robustness and consistency of threshold relationships between area burned and FM and the consequent capability to adequately monitor spatiotemporal variations in FM across large-scale bioclimatic gradients. Currently, robust methods for estimating FM dynamics at relevant scales remain limited [*Yebra et al*., 2013], and the robustness of the threshold relationships between both dead and live FM and area burned by wildfires therefore remains largely unexplored across large bioclimatic gradients. A notable exception is *Jurdao et al*. [2012] who examined relationships between live FM, estimated from satellite observations, and fire occurrence across 492,175 km^2 of the Iberian Peninsula in Spain. Integration of dynamic changes to the moisture content of both live (e.g., green foliage) and dead fuels is also required to be able to predict the potential for major wildfire events.

In this study, we test the hypothesis that the area burned by wildfires at the regional or subcontinental scale is governed by discrete FM thresholds. We also test whether such thresholds are robust across major variations in climatic and vegetation groups. We examined recent wildfires in eucalypt forests and woodlands across southeastern Australia, a region prone to major wildfires, and concurrent spatial patterns of FM, using recently developed methods for macroscale, spatially explicit prediction of both live [*Caccamo et al*., 2012b] and dead FM [*Nolan et al*., 2016]. The study is novel as it (i) provides the first test at a subcontinental-scale of whether the area burned by wildfire is governed by thresholds in both dead and live FM and (ii) provides an assessment of the capacity for monitoring and assessing wildfire risk using remotely sensed or modeled estimates of both live and dead FM.

2. Materials and Methods

2.1. Study Area

The study area incorporates forests and woodlands across 117,059 km^2 of southeastern Australia (Figure 1 a). There is a broad climate gradient within the study area, which extends for 760 km from north to south and from sea level to over 2000 m in altitude. Across the study area average annual precipitation ranges from 600 to 3000 mm, and average daily temperature ranges from 6 to 18°C [*Bureau of Meteorology*, 2013]. Wildfires generally occur from early spring to early autumn, with the period of peak fire activity moving progressively south over this period as a function of cold frontal activity [*Hasson et al*., 2009]. We divided the study area into two distinct zones based on seasonal rainfall patterns, modified from the agro-climate classification of *Hutchinson et al*. [2005]. The eastern climate zone has rainfall distributed throughout the year, while the western climate zone has rainfall predominately in winter or spring, with drier summers (Figure 1b). Vegetation was classified as either eucalypt forest or eucalypt woodland, with either a grassy, shrubby, or wet understory (i.e., six vegetation groups in total; Table 1). Vegetation was identified from the major vegetation groups of the National Vegetation Information System, version 4.1 (http://www.environment.gov.au).

2.2. Area Burned

Fire history data sets were obtained from the Victorian Department of Environment, Land, Water and Planning and from the New South Wales Rural Fire Service. These data sets consist of polygons of the areas burnt by wildfire and the start date of the fire. The study period covers the 2000 to 2013 fire seasons, with a fire season spanning from July to the following June (i.e., the 2000 fire season runs from July 2000 to June 2001). This period was chosen because the total area burned was exceptional in recent history (39,642 km^2; Figure 1b) [*Bradstock et al*., 2014] and high-resolution climatic data and reliable remote sensing imagery, i.e., Moderate Resolution Imaging Spectroradiometer (MODIS), were available.

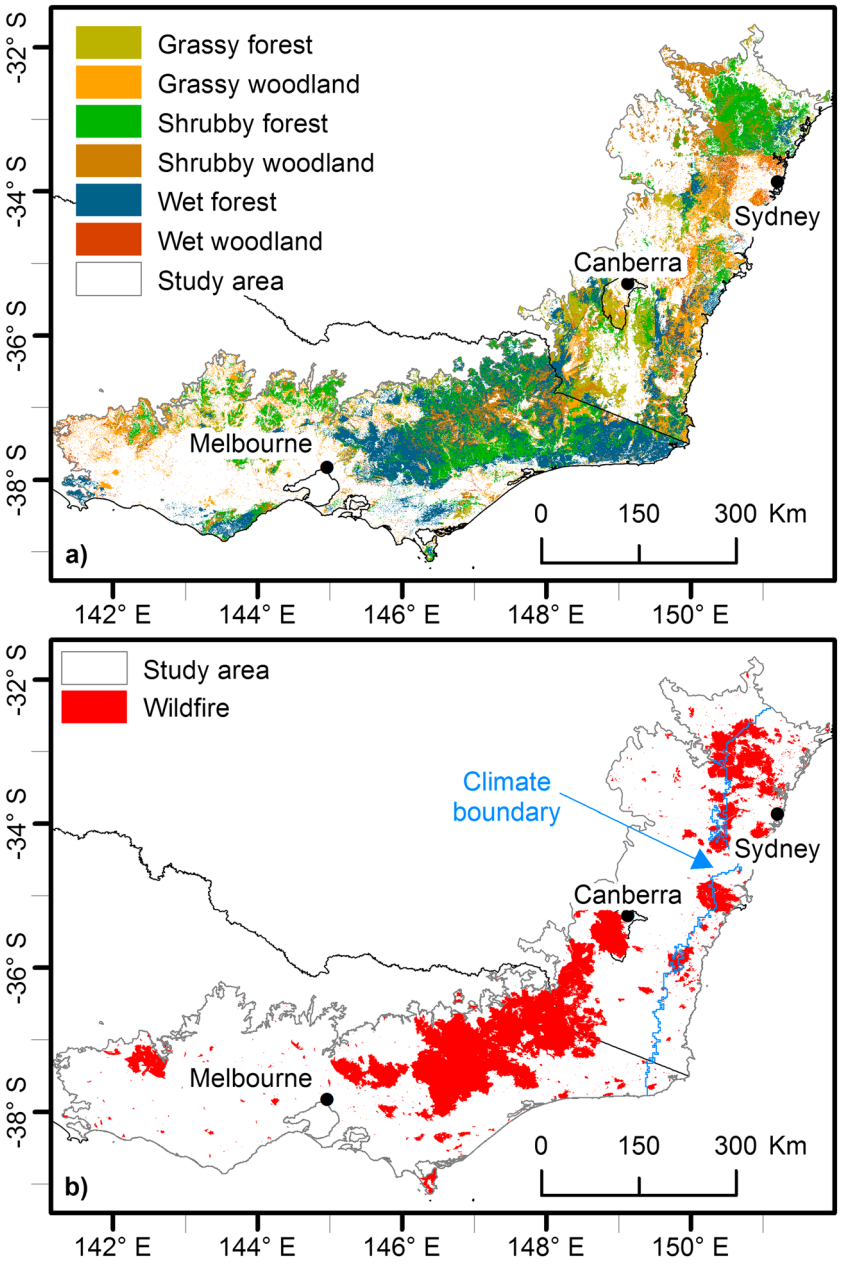

Figure 1. Map of the study area in southeastern Australia showing (a) the extent of the vegetation groups used in this study and (b) the extent of wildfires in the study area dating from the 2000–2013 fire seasons and the climate boundary delineating different precipitation patterns. Vegetation data were obtained from the National Vegetation Information System; fire history data sets obtained from the Victorian Department of Environment, Land, Water and Planning and from the New South Wales Rural Fire Service; and the climate boundary modified from *Hutchinson et al.* [2005] separating the region with uniform or summer precipitation to the east, from that with winter or spring precipitation to the west.

2.3. Dead Fuel Moisture

Dead FM was estimated for suspended fuels in the 10 h fuel class (6.35–25 mm diameter) from a semimechanistic model originally developed by *Resco de Dios et al.* [2015] and with its spatial application developed by *Nolan et al.* [2016]. Although we focus on 10 h fuels here, moisture content of fuels in the finer, 1 h class (litter <6.35 mm) is related to 10 h FM [*Resco de Dios et al.*, 2015]. The dead FM model is based on an exponential relationship between moisture content and vapor pressure deficit, D [*Nolan et al.*, 2016]:

$$\text{Dead FM}\ (\%) = 6.79 + 27.43e^{(-1.05\ D)} \quad (1)$$

Table 1. Description of the Study Area

Study Area	Description	Total Area (km^2)	Area Burnt (km^2)
Entire study area	Forests and woodlands across southeastern Australia	117,059	39,642
Study area divided by climate zone			
Eastern zone	Rainfall distributed throughout the year	97,221	35,108
Western zone	Rainfall occurs predominately in winter or spring, with drier summers	19,838	4,533
Study area divided by vegetation group			
Grassy forest	*Eucalyptus* open forests with a grassy understorey	13,430	3,722
Shrubby forest	*Eucalyptus* open forests with a shrubby understorey	29,998	11,817
Wet forest	*Eucalyptus* open forests with tree ferns, sedges, rushes, or wet tussock grassland	34,768	12,946
Grassy woodland	*Eucalyptus* woodlands with a grassy understorey, including tussock and hummock grasses	20,214	3,241
Shrubby woodland	*Eucalyptus* woodlands with a shrubby or chenopod understorey	15,152	7,399
Wet woodland	*Eucalyptus* woodlands with ferns, sedges, rushes, or wet tussock grassland	3,497	517

D was obtained from the SILO climate database (http://www.longpaddock.qld.gov.au/silo/index.html). SILO climate data are estimated from interpolated weather station measurements and are available across Australia on a regular 0.05° grid [*Jeffrey et al*., 2001].

2.4. Live Fuel Moisture

Live FM was estimated with data products from the MODIS Terra satellite, following the methods of *Caccamo et al*. [2012b], and recalibrated using field observations across a wider range of environmental conditions (Table S1 in the supporting information). The Visible Atmospherically Resistant Index (VARI) and Normalized Difference Infrared Index (NDIIb6) were calculated from the MODIS 8 day composite data set MOD09A1 (collection 5), with a 500 m spatial resolution. We used only these indices because they were the ones that best corresponded with live FM data in *Caccamo et al*. [2012b]. Data anomalies in MOD09A1, including cloud cover, were masked using MODIS quality assurance layers. VARI was calculated as (band 4 − band 1)/(band 4 + band 1 − band 3) [*Gitelson et al*., 2002]. NDIIb6 was calculated as (band 2 − band 6)/(band 2 + band 6) [*Hunt and Rock*, 1989; *Jackson et al*., 2004]. For each spectral index (SI; i.e., VARI and NDIIb6), a normalization approach was applied, whereby the relative variation of a pixel at a given time compared to the minimum and maximum value observed for that pixel over the image time series (February 2000–December 2014) was calculated as

$$SI_{max-min\ i} = \left(\frac{SI_i - SI_{min}}{SI_{max} - SI_{min}}\right) \quad (2)$$

where $SI_{max-min\ i}$ is the normalized SI of a given pixel at time *i*, SI_i is the SI at time *i*, and SI_{min} and SI_{max} are the minimum and maximum observed values of the SI for the time series of images analyzed [*Chuvieco et al*., 2002; *Stow and Niphadkar*, 2007]. Pixels were excluded from analyses if wildfire had occurred in the previous 5 years, since this is the length of time after which fire alters the spectral reflectance of vegetation [*Caccamo et al*., 2012a].

The live FM model of *Caccamo et al*. [2012b] predicted live FM values between 86 and 127%. FM is a ratio of the mass of water within a fuel sample to the oven-dry weight of that fuel [*Chuvieco et al*., 2002]. We recalibrated and tested this model with live FM data collected across a larger region and a larger range of moisture values (65–188%). Further details on these methods are provided in Text S1 in the supporting information.

2.5. Data Analyses

2.5.1. Critical Fuel Moisture Thresholds

For each wildfire footprint we calculated the median value of dead and live FM across the footprint, and separately for each of the climate zones, and again for each of the vegetation groups found within that footprint. Median FM was calculated for both dead and live fuels (due to the non normal distribution of FM; Figure S3 in the supporting information). For dead fuels, calculations were undertaken with daily time step data for the

recorded start date of the fire. While for live fuels FM was calculated with 8 day composite data for the period immediately preceding the start date, because fire alters spectral reflectance properties. Although some wildfires may burn for several days to weeks, only start date information is recorded in the fire history data set. We then calculated the cumulative area burnt by wildfire as a function of FM, following *Dennison* and *Moritz* [2009]. Briefly, segmented regression was used to fit linear regressions to either side of breakpoints in the regressions between FM and cumulative area burnt by wildfire. The number of breakpoints included in the regression was determined by progressively increasing the number of breakpoints used in fitting the model. Akaike's information criterion (AIC) [*Akaike*, 1974] was calculated for each model, and the model with the lowest AIC was selected [*Burnham and Anderson*, 2002].

2.5.2. Temporal Dynamics of Fuel Moisture and Area Burned

Temporal dynamics in FM and area burned were identified across a dry (2006/2007) and a wet (2010/2011) fire season. For each day of the fire season, median dead FM and total area burned were calculated across all forest and woodland types, while live FM was calculated using sequential 8 day data. Separate analyses of fuel dryness and area burned were undertaken for each of the two climate zones.

All analyses were undertaken in R [*R Development Core Team*, 2015] using the raster [*Hijmans*, 2013], shapefiles [*Stabler*, 2013], and segmented [*Muggeo*, 2003] packages.

3. Results

3.1. Live Fuel Moisture Model Calibration

For both $VARI_{max-min}$ and $NDIIb6_{max-min}$, an exponential model fitted the calibration data set ($n = 43$) better than a linear model. For $VARI_{max-min}$ $r^2 = 0.61$ and 0.63 for the linear and exponential models respectively; for $NDIIb6_{max-min}$ $r^2 = 0.03$ and 0.05. The exponential model was statistically significant for $VARI_{max-min}$ ($p < 0.001$) but not $NDIIb6_{max-min}$ ($p = 0.14$). Thus, the following $VARI_{max-min}$ model was used for subsequent calculations of live FM:

$$\text{Live FM}\ (\%) = 52.51\, e^{1.36\ VARI_{max-min}} \tag{3}$$

Validation of this model ($n = 30$) showed it to perform well, with observed FM values being only slightly underpredicted: mean absolute error = 9.5%, mean bias error = −7.1%, and $r^2 = 0.69$ (Figure S3 in the supporting information), with one outlier (observed FM = 189%) with a Cook's D of 2.2 excluded.

3.2. Critical Fuel Moisture Thresholds

The relationships between area burned and both live and dead FM were nonlinear, with steep rises in area burned evident once FM fell below threshold values (Figure 2). Across the entire study area, there were two thresholds identified for live FM that demarcated a major increase in area burned. The first was at 156.1% (95% CI: 152.6–159.6%) while the second was at 101.5% (95% CI: 100.9–101.8%; Figure 2a). This represents 99.9% and 78.5% of the total area burnt, for each threshold, respectively. There was an additional threshold identified at 72.4% (95% CI: 71.89–72.8%), but this was not associated with increasing area burned (i.e., the slope of the regression line was shallower than between the live FM values of 152.6–101.5%). Similarly, there were two thresholds identified for dead FM across the entire study area that demarcated a major increase in area burned. The first was at 14.6% (95% CI: 14.5–14.7%) while the second was at 9.9% (95% CI: 9.8–10.1; Figure 2b). This represents 96.9% and 53.7% of the total area burnt, for each threshold, respectively.

When the analysis was repeated for each of the two climate zones separately, we found that the western climate zone had critical thresholds of live FM that were similar to those previously identified: 155.6% (95% CI: 155.4–159.8%) and 101.5% (95% CI: 100.9–102.1%; Figure 2c). However, the eastern climate zone had significantly lower thresholds (i.e., confidence intervals did not overlap): 113.6% (95% CI: 113.0–114.3%) and 81.6% (95% CI: 81.5–81.76%; Figure 2d). For dead FM, although the two climate zones had significantly different thresholds, these values were quite close to each other, particularly for the threshold at the wetter end of FM: 15.1% (95% CI: 14.7–15.7%) and 14.2% (95% CI: 14.1–14.3%) for the eastern and western climate zones, respectively, and for the drier threshold: 8.2% (95% CI: 8.2–8.2%) and 6.9% (95% CI: 6.9–6.9%) for the eastern and western climate zones, respectively (Figure 2d).

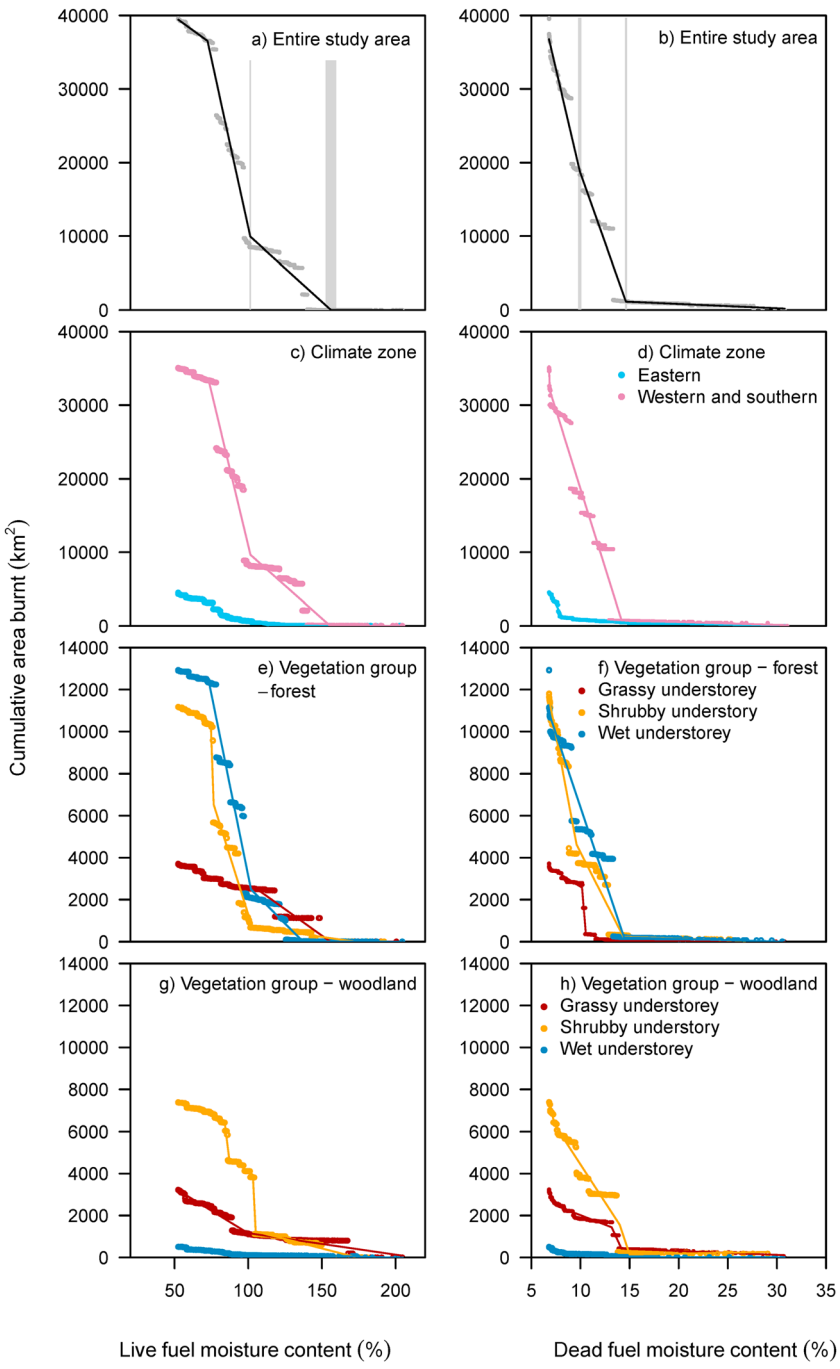

Figure 2. Relationship between live and dead fuel moisture and cumulative areas burnt by wildfire. Fuel moisture is the median value calculated across the footprint for a given fire event. Fitted to the data are segmented regressions which identify fuel moisture thresholds demarcating a substantial increase in fire activity. (a and b) The vertical grey bars represent the 95% CI of critical FM thresholds; (c–h) for clarity, these are not presented. The r^2 values for each of the segmented regressions were all ≥0.96.

For the differing vegetation groups, all had a live FM threshold similar to the 101.5% identified across the entire study area: 98.5–105.9% (Figures 2e and 2g). However, the live FM threshold at the wetter range of FM values was more variable across the different vegetation groups: 136.9–167.8%, and in the case of shrubby forests and shrubby woodlands, no wetter threshold was identified at all. For dead FM, all vegetation groups had a similar FM threshold at the wetter range of values: 12.4–15.0% (Figures 2f and 2g). There was

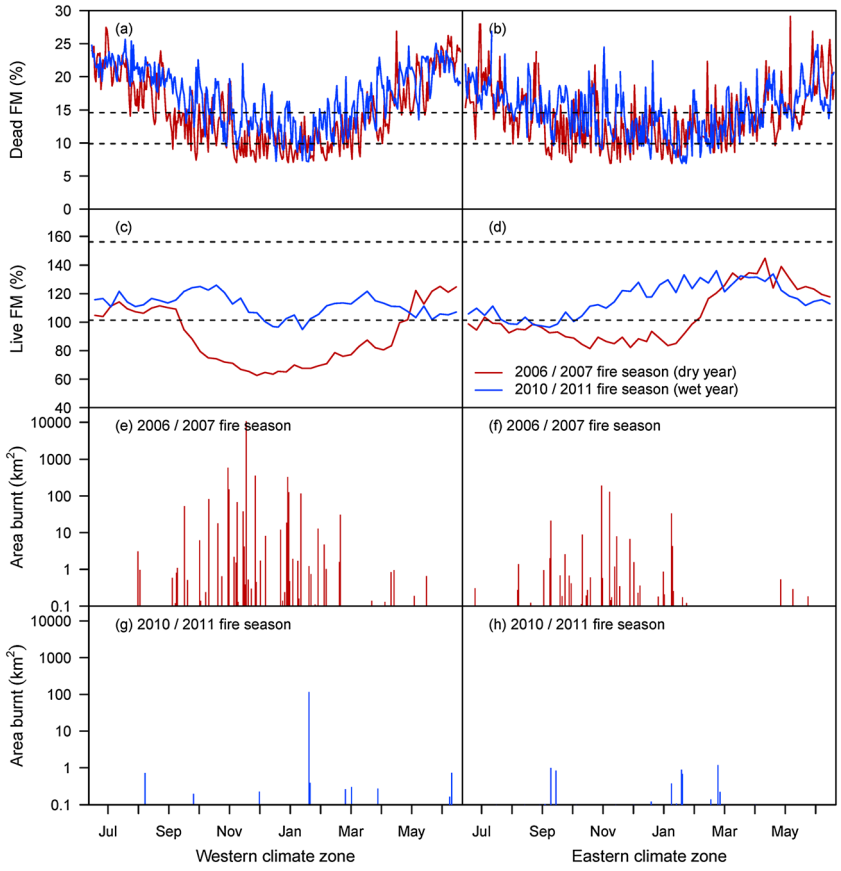

Figure 3. Median values of (a and b) dead FM and (c and d) live FM and (e–h) area burnt by wildfire over a dry year (2006/2007 fire season) and a wet year (2010/2011 fire season). Data are divided into the two different climate zones due to differences in timing of wildfires between the two climate zones. Also shown are the dead and live FM thresholds calculated from segmented regression. These thresholds were calculated across the entire study area.

also a similar threshold identified across the vegetation groups at the drier end of dead FM values: 7.4–8.9%, except for wet forests, where only one threshold was identified.

3.3. Temporal Dynamics of Fuel Moisture and Area Burned

As expected for both dead and live fuels, FM thresholds were reached more frequently during the dry year of 2006/2007 than for the wet year of 2010/2011, and lower FM was associated with greater fire activity (Figure 3). While small fires (<1 km^2) occurred throughout 2006/2007, larger fires were associated with the periods when both dead and live FM were below identified thresholds.

Day-to-day variation in dead FM was high, as expected. For example, during both the wet and dry fire seasons, dead FM crossed from a wet state above the upper threshold (14.6%) to below the lower threshold (9.9%), within a week. FM transformations were slower for live fuels, though could still occur over a period of weeks. For example, during the dry year FM changed from 109% to 75% (well below the lower threshold of 101.5%) over 4 weeks (Figure 3c). Changes in live FM occurred more rapidly when FM was in the recovery, rather than drying, phase. For example, recovery of moisture content in live fuels occurred more rapidly, with FM increasing from 83% to 122% over a 24 day time period (Figure 3c).

4. Discussion and Conclusions

The occurrence of wildfire in forests and woodlands across southeastern Australia was clearly associated with the incidence of critical thresholds of macroscale, mean live and dead FM during the 2000 to 2013 fire seasons (Figure 2). The first major novel outcome of this study was the formal demonstration that dynamic

transformations in FM associated with major wildfires can occur rapidly for dead fuels and within several weeks to months for live fuels (Figure 3). Therefore, relatively small changes in FM close to these thresholds, across landscapes, can transform the potential for major wildfires in these vegetation types, consistent with the switch hypothesis proposed by *Bradstock* [2010]. The second major novel outcome of this study was the confirmation of the capacity to monitor such critical, rapid transformations in wildfire potential via remote sensing and climatic modeling. This, combined with the potential to forecast *D*, and thus dead FM, provides a significant new capacity for monitoring FM to assist in operational planning and risk assessment for major wildfires that is robust across major climatic and vegetation gradients at a subcontinental scale.

4.1. Critical Thresholds of Fuel Moisture

For dead fuels, we found that small wildfires ($<$0.15 km^2; Figure 2) occurred with FM as high as 30.8% (Figure 2b), which is consistent with previously reported moisture of extinction (ME) values of 25–35% for woody fuel [*Burgan and Rothermel*, 1984; *Fernandes et al*., 2008; *Rothermel*, 1972]. Remarkably, the wetter dead FM threshold of 12.4–15.1% (which represents the thresholds calculated across all analyses) is similar to thresholds found in subalpine and boreal forests in North America, where dead FM below 14% was associated with increased probability of lightning strikes initiating fire [*Nash and Johnson*, 1996]. This threshold corresponded to a *D* of 1.1–1.5 kPa in our study, similar to that found by *Williams et al*. [2015] who showed that annual area burned in southwestern U.S. forests increased rapidly when *D* was between 1.3 and 1.4 kPa. This suggests that this threshold value of dead FM is applicable across forests and woodlands generally and not just in the eucalypt forests and woodlands used in this study. This is consistent with our use of a dead FM model based on *D*, which was found to be robust across different woody vegetation types in Australia and California [*Nolan et al*., 2016; *Resco de Dios et al*., 2015]. The second threshold of dead FM (6.9–9.9%) represents a further increase in the rate of area burnt with declining FM and is also associated with an increase in the occurrence of large fire events.

For live fuels, we found that small fires occurred with FM as high as 205%. This is similar to shrublands, where the upper value of live FM that supports wildfire has been reported at 200% and 211% in some studies [*Chuvieco et al*., 2009; *Schoenberg et al*., 2003], although lower values have also been reported: 160–170% [*Dennison* and *Moritz*, 2009; *Jurdao et al*., 2012]. The first live FM threshold (113.6–167.8%), although highly variable across climate zones and vegetation groups, is consistent with similar research in shrublands, where burn area increases substantially faster when live FM declines below 140% [*Schoenberg et al*., 2003]. The second live FM threshold (98.5–105.9%) is similar to results reported elsewhere for forests, with live FM thresholds of between 100 and 120% identified for Pacific Northwest conifer forests [*Agee et al*., 2002]. Thresholds reported for shrublands are generally lower: 79–111% [*Chuvieco et al*., 2009; *Dennison* and *Moritz*, 2009; *Dennison et al*., 2008]. The slightly higher thresholds found in this study compared to shrublands may be a function of the relatively high inherent flammability of the tree foliage in the *Eucalyptus*-dominated woodlands and forests of our study area. *Dimitrakopoulos* and *Papaioannou* [2001] also reported a higher ME for *Eucalyptus camaldulensis* ($>$140%), compared to other common Mediterranean fuels. Additionally, forests and woodlands typically occur in wetter parts of the landscape than shrublands and therefore are likely to have higher live FM compared to shrublands, even when dead FM is critically low and ambient weather is conducive to the rapid spread of fire.

In general, with the exception of some restricted wet vegetation types, the live and dead threshold FM values found in our study may have reflected the large sampling scales which inherently aggregate moisture values across diverse terrain and vegetation variations within the broad vegetation types. Continuity of dry patches is required to provide the potential for large fires [*Caccamo et al*., 2012a]. For this to occur, many parts of the landscape that are normally moist (e.g., shaded slopes and gullies) must dry out (e.g., FM must fall below ME). While this drying is occurring, FM in other parts of the landscape, such as ridges and north facing slopes, may reach levels considerably lower than hypothetical ME values. Thus, the FM thresholds reported here were likely to reflect these dynamics and variability.

At the wetter range of FM values, we found that FM thresholds were inconsistent across climate zones and vegetation groups. This is likely a function of the differing data set sizes, rather than a reflection of any inherent differences between live fuels across climate zones or vegetation groups. For example, for woodlands with a wet understorey, which represented the smallest data set (only 1.3% of the total area of fires sampled), we identified three distinct FM thresholds from segmented regression for both live and dead fuels. However,

the increase in fire activity across FM thresholds was only marginal, particularly when compared with other vegetation groups (Figures 2g and 2h). This highlights a limitation of this approach to identifying FM thresholds, with smaller data sets likely to generate less accurate estimates of FM thresholds than larger data sets, as expected from statistical first principles.

4.2. Temporal Dynamics of Fuel Moisture and Area Burned

The moisture content of fine, suspended, dead fuels is driven by ambient atmospheric conditions. As a result, dead FM can rapidly transform from a wet to dry state. In contrast, live fuels dry out more slowly, in response to declining soil moisture. Because of these temporal differences in wetting and drying cycles, dead fuels are more consistently available to burn over the summer months, while the availability of live fuels shows greater interannual variability, coincident with wildfire activity (Figure 3). Thus, critical moisture values of dead fuels may be considered the first necessary precondition, or switch, that must be activated for wildfires to occur, followed by critical moisture values of live fuels. Further, the calculated live FM thresholds are likely to be dependent to some extent on dead FM. For example, if dead FM is low enough to ignite a fire, the fire may not be sustained if live FM is above critical values. These potential interdependencies between fuel components are worthy of examination in future studies. By examining live and dead FM separately we are maximizing the potential for other uses of this approach. For example, land managers may target prescribed burning ignitions for when dead FM is low enough to burn litter but live FM high enough that the fire does not spread into the crown. This could also be examined in future studies.

While the moisture content of fuels is clearly an important precondition for fire occurrence, it may not be the most important, particularly given that dead FM can remain below critical threshold values for several months of the year. The occurrence of weather conditions conducive to the rapid spread of fire and the occurrence of ignitions are also necessary switches that must occur in order to exploit the potential for large wildfires provided by landscape-level templates of highly continuous dry fuels.

Although live fuels dry out more slowly than dead fuels, live FM can still move across critical thresholds of FM in as little as a month (Figure 3 [*Caccamo et al.*, 2012a]). This demonstrates the importance of monitoring live FM at high temporal resolution to detect shifts in moisture content. Here we demonstrated the capacity of MODIS 8 day composite data to detect such shifts. This, combined with daily time step climatic data for calculating dead FM, has the potential to immediately improve fire risk assessments in forests and woodlands globally. Moreover, the approach presented here can be readily used within Earth system models to examine future climate variability and associated fire risk.

Acknowledgments
We would like to thank R. Gibson, M. Chick, D. Spencer, S. Khanal, A. Boer-Cueva, L. Serrano-Grijalva, D. Bridgman, and C. Beattie for their invaluable assistance in collecting fuel moisture data. We also thank two anonymous reviewers for their useful comments on the draft manuscript. This project was funded by Victorian Department of Environment, Land, Water and Planning via the Bushfire Cooperative Research Centre, grants from the Hawkesbury Institute for the Environment and a Ramón y Cajal Fellowship to VRD (RYC-2012-10970). MODIS data products were courtesy of the online Data Pool at the NASA Land Processed Distributed Archive Centre, USGS/Earth Resources Observation and Science Center, Sioux Falls, SD (https://lpdaac.usgs.gov/data_access).

References

Agee, J. K., C. S. Wright, N. Williamson, and M. H. Huff (2002), Foliar moisture content of Pacific Northwest vegetation and its relation to wildland fire behavior, *For. Ecol. Manage.*, *167*(1-3), 57–66.

Akaike, H. (1974), A new look at statistical model identification, *IEEE Trans. Autom. Control*, *AC19*(6), 716–723.

Aragao, L., Y. Malhi, R. M. Roman-Cuesta, S. Saatchi, L. O. Anderson, and Y. E. Shimabukuro (2007), Spatial patterns and fire response of recent Amazonian droughts, *Geophys. Res. Lett.*, *34*, doi:10.1029/2006GL028946.

Bradshaw, L., J. Deeming, R. E. Burgan, and J. Cohen (1983), The 1978 National Fire-Danger Rating System: Technical documentation GTR-INT-169, USDA, Forest Service, Ogden, Utah.

Bradstock, R., T. Penman, M. Boer, O. Price, and H. Clarke (2014), Divergent responses of fire to recent warming and drying across south-eastern Australia, *Global Change Biol.*, *20*(5), 1412–1428.

Bradstock, R. A. (2010), A biogeographic model of fire regimes in Australia: Current and future implications, *Global Ecol. Biogeogr.*, *19*(2), 145–158.

Bureau of Meteorology (2013), Climate data online edited, Australian Government.

Burgan, R. E., and R. C. Rothermel (1984), BEHAVE: Fire Behavior Prediction and Fuel Modeling System Fuel Subsystem, USDA Forest Service, GTR INT-167, Ogden, Utah.

Burnham, K. P., and D. R. Anderson (2002), *Model Selection and Multi/Model Inference: A Practical Information-Theoretic Approach*, Springer, New York.

Caccamo, G., L. A. Chisholm, R. A. Bradstock, and M. L. Puotinen (2012a), Using remotely-sensed fuel connectivity patterns as a tool for fire danger monitoring, *Geophys. Res. Lett.*, *39*, doi:10.1029/2011GL050125.

Caccamo, G., L. A. Chisholm, R. A. Bradstock, M. L. Puotinen, and B. G. Pippen (2012b), Monitoring live fuel moisture content of heathland, shrubland and sclerophyll forest in south-eastern Australia using MODIS data, *Int. J. Wildland Fire*, *21*(3), 257–269.

Chuvieco, E., D. Riano, I. Aguado, and D. Cocero (2002), Estimation of fuel moisture content from multitemporal analysis of Landsat Thematic Mapper reflectance data: Applications in fire danger assessment, *Int. J. Remote Sens.*, *23*(11), 2145–2162.

Chuvieco, E., I. Gonzalez, F. Verdu, I. Aguado, and M. Yebra (2009), Prediction of fire occurrence from live fuel moisture content measurements in a Mediterranean ecosystem, *Int. J. Wildland Fire*, *18*(4), 430–441.

Dennison, P. E., and M. A. Moritz (2009), Critical live fuel moisture in chaparral ecosystems: A threshold for fire activity and its relationship to antecedent precipitation, *Int. J. Wildland Fire*, *18*(8), 1021–1027.

Dennison, P. E., M. A. Moritz, and R. S. Taylor (2008), Evaluating predictive models of critical live fuel moisture in the Santa Monica Mountains, California, *Int. J. Wildland Fire*, *17*(1), 18–27.

Dimitrakopoulos, A. P., and K. K. Papaioannou (2001), Flammability assessment of Mediterranean forest fuels, *Fire Technol.*, *37*(2), 143–152.
Dowdy, A. J., and G. A. Mills (2012), Atmospheric and fuel moisture characteristics associated with lightning-attributed fires, *J. Appl. Meteorol. Climatol.*, *51*(11), 2025–2037.
Fernandes, P. M., H. Botelho, F. Rego, and C. Loureiro (2008), Using fuel and weather variables to predict the sustainability of surface fire spread in maritime pine stands, *Can. J. For. Res.-Rev. Can. Rech. For.*, *38*(2), 190–201.
Gitelson, A. A., R. Stark, U. Grits, D. Rundquist, Y. Kaufman, and D. Derry (2002), Vegetation and soil lines in visible spectral space: A concept and technique for remote estimation of vegetation fraction, *Int. J. Remote Sens.*, *23*(13), 2537–2562.
Hasson, A. E. A., G. A. Mills, B. Timbal, and K. Walsh (2009), Assessing the impact of climate change on extreme fire weather events over southeastern Australia, *Clim. Res.*, *39*(2), 159–172.
Hijmans, R. J. (2013), Raster: Geographic data anaysis and modeling, R package version 2.1-62/r2833. [Available at http://R-Forge.R-project.org/projects/raster/.]
Hunt, E. R., and B. N. Rock (1989), Detection of changes in leaf water content using near-infrared and middle-infrared reflectances, *Remote Sens. Environ.*, *30*(1), 43–54.
Hutchinson, M. F., S. McIntyre, R. J. Hobbs, J. L. Stein, S. Garnett, and J. Kinloch (2005), Integrating a global agro-climatic classification with bioregional boundaries in Australia, *Global Ecol. Biogeogr.*, *14*(3), 197–212.
Jackson, T. J., D. Y. Chen, M. Cosh, F. Q. Li, M. Anderson, C. Walthall, P. Doriaswamy, and E. R. Hunt (2004), Vegetation water content mapping using Landsat data derived normalized difference water index for corn and soybeans, *Remote Sens. Environ.*, *92*(4), 475–482.
Jeffrey, S. J., J. O. Carter, K. M. Moodie, and A. R. Beswick (2001), Using spatial interpolation to construct a comprehensive archive of Australian climate data, *Environ. Model. Software*, *16*(4), 309–330.
Jurdao, S., E. Chuvieco, and J. M. Arevalillo (2012), Modelling fire ignition probability from satellite estimates of live fuel moisture content, *Fire Ecol.*, *8*(1), 77–97.
McArthur, A. G. (1967), *Fire Behaviour in Eucalypt Forests*, *Leaflet*, vol. 107, Department of National Development Forestry and Timber Bureau, Canberra.
Meyn, A., P. S. White, C. Buhk, and A. Jentsch (2007), Environmental drivers of large, infrequent wildfires: The emerging conceptual model, *Prog. Phys. Geogr.*, *31*(3), 287–312.
Moritz, M. A., et al. (2014), Learning to coexist with wildfire, *Nature*, *515*(7525), 58–66.
Muggeo, V. M. R. (2003), Estimating regression models with unknown break-points, *Stat. Med.*, *22*, 3055–3071.
Nash, C. H., and E. A. Johnson (1996), Synoptic climatology of lightning-caused forest fires in subalpine and boreal forests, *Can. J. For. Res.-Rev. Can. Rech. For.*, *26*(10), 1859–1874.
Nolan, R. H., V. Resco de Dios, M. M. Boer, G. Caccamo, M. L. Goulden, and R. A. Bradstock (2016), Predicting dead fine fuel moisture at regional scales using vapour pressure deficit from MODIS and gridded weather data, *Remote Sens. Environ.*, *174*, 100–108.
O'Donnell, A. J., M. M. Boer, W. L. McCaw, and P. F. Grierson (2011), Climatic anomalies drive wildfire occurrence and extent in semi-arid shrublands and woodlands of southwest Australia, *Ecosphere*, *2*(11), 15.
R Development Core Team (2015), R: A language and environment for statistical computing, R Foundation for Statistical Computing, Vienna, Austria. [Available at http://www.R-project.org/.]
Resco de Dios, V., A. W. Fellows, R. H. Nolan, M. M. Boer, R. A. Bradstock, F. Domingo, and M. L. Goulden (2015), A semi-mechanistic model for predicting the moisture content of fine litter, *Agric. For. Meteorol.*, *203*, 64–73.
Rothermel, R. C. (1972), A mathematical model for predicting fire spread in wildland fuels edited by F. S. USDA, Res. Pap. INT-115, Ogden, Utah.
Schoenberg, F. P., R. Peng, Z. J. Huang, and P. Rundel (2003), Detection of non-linearities in the dependence of burn area on fuel age and climatic variables, *Int. J. Wildland Fire*, *12*(1), 1–6.
Sharples, J. J. (2009), An overview of mountain meteorological effects relevant to fire behaviour and bushfire risk, *Int. J. Wildland Fire*, *18*(7), 737–754.
Stabler, B. (2013), Read and write ESRI shapefiles R package version 0.7.
Stow, D., and M. Niphadkar (2007), Stability, normalization and accuracy of MODIS-derived estimates of live fuel moisture for Southern California chaparral, *Int. J. Remote Sens.*, *28*(22), 5175–5182.
Turner, D., B. Ostendorf, and M. Lewis (2008), An introduction to patterns of fire in arid and semi-arid Australia, 1998-2004, *Rangeland J.*, *30*(1), 95–107.
Van Wagner, C. E. (1987), Development and structure of the Canadian Forest Fire Weather Index System Tech. Rep., 35 pp., Canadian Forestry Service, Ottawa, Ont.
Verdon, D. C., A. S. Kiem, and S. W. Franks (2004), Multi-decadal variability of forest fire risk—Eastern Australia, *Int. J. Wildland Fire*, *13*(2), 165–171.
Viegas, D. X., M. T. Viegas, and A. F. Ferreira (1992), Moisture content of fine forest fuels and fire occurrence in central Portugal, *Int. J. Wildland Fire*, *2*(2), 69–86.
Williams, A. P., et al. (2015), Correlations between components of the water balance and burned area reveal new insights for predicting forest fire area in the Southwest United States, *Int. J. Wildland Fire*, *24*(1), 14–26.
Yebra, M., P. E. Dennison, E. Chuvieco, D. Riano, P. Zylstra, E. R. Hunt, F. M. Danson, Y. Qi, and S. Jurdao (2013), A global review of remote sensing of live fuel moisture content for fire danger assessment: Moving towards operational products, *Remote Sens. Environ.*, *136*, 455–468.